

# Thin Films of Perpendicularly Oriented Diblock Copolymers: Lamellar Distortions Driven by Surface–Diblock Interfacial Tensions

G. G. Pereira<sup>\*,†,‡</sup> and D. R. M. Williams<sup>†</sup>

Department of Applied Mathematics, Research School of Physical Sciences and Engineering, Australian National University, Canberra ACT, 0200, Australia, and School of Chemistry, University of Sydney, NSW 2006, Australia

Received July 16, 1998; Revised Manuscript Received October 26, 1998

**ABSTRACT:** We consider the problem of a diblock copolymer melt thin film on a homogeneous flat surface or confined between two flat plates. When there is significant mismatch between the film thickness and an integer multiple of the lamellar spacing, perpendicular orientation of the lamellae may be observed. However, because of differences in the interfacial tensions between the surface and the two blocks, the lamellae may be distorted, from a straight interface to a curved interface. We examine theoretically this distortion and show that its amplitude may only be a few percent of the lamellar spacing.

## 1 Introduction

One problem of current interest is the behavior of thin films of diblock copolymers placed on a solid surface.<sup>1–8</sup> These diblocks self-assemble in bulk to form various morphologies. The simplest form, and the one we will consider here, is the lamellar phase formed from symmetric diblocks. In the bulk, there is a preferred bilayer spacing,  $L_2$ . In a thin film, the diblocks will usually be unable to achieve this preferred spacing and will be frustrated because of confinement. This frustration can induce a change in the orientation of the lamellae from being parallel to the substrate to being perpendicular to it.<sup>2</sup> The perpendicular orientation reduces the amount of stretching and interface between the two blocks. However, usually one of the blocks will have a preference for lying at the upper or lower bounding surfaces. In the parallel orientation, this preference can be accommodated, but in the perpendicular orientation, both blocks make equal contact with both bounding surfaces. This is energetically unfavorable, and we might expect that the perpendicular orientation would be subject to the instability depicted (side-on) in Figure 1b. In this situation, the *A* block prefers to lie at the upper surface and the *B* block at the lower surface. The lamellae distort to allow for this preference. In this paper, we analyze quantitatively this instability. We show that in all cases of perpendicular alignment the instability will exist but that it is always of very small amplitude; i.e., the increase in area devoted to one or other of the blocks at either surface is at most a few percent. This has implications for the case for which one wants to produce the perpendicular orientation. One example is in the production of lithographic templates.<sup>9</sup> Our study shows that the uniformity of the pattern at the surface should always be very high. In the following, we describe the calculation, give some examples of the distortion pattern, and compare the distorted perpendicular orientation with the parallel orientation.

## 2 Model Description

We begin by examining lamellae in the perpendicular orientation seen side-on in Figure 1a. Consider a single

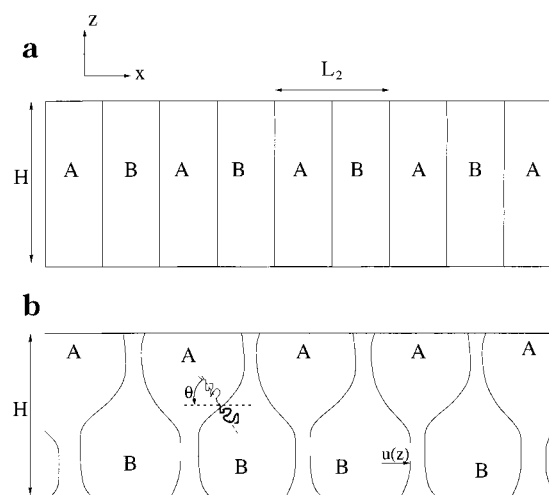


**Figure 1.** (a) Side view of a schematic of the thin film melt with the undistorted lamellae orientated perpendicular to the flat surface. The  $y$  direction is perpendicular to the page. (b) Possible deformation that may occur for the lamellar interfaces of the diblock copolymer melt. We assume *A* blocks prefer the upper surface compared to *B* blocks. This schematic is for  $\Delta g_s > 0$ , although in this study we consider any  $\Delta g_s$ .

*AB* lamella which is of infinite extent in the  $y$  direction and of thickness  $H$  in the  $z$  direction (normal to the surface). The lamella is made up of diblocks with  $2N$  monomers in total, each of size  $a$ . The bulk equilibrium spacing of an *AB BA* bilayer<sup>10</sup> is

$$L_2 = 4(6\gamma_{AB}a^5/\pi^2k_B T)^{1/3} N^{2/3} \quad (1)$$

where  $\gamma_{AB}$  is the *AB* interfacial tension and  $T$  is the temperature. The lamella's orientation is perpendicular to the surface and has a spacing  $L_2/2$ ; i.e., it is half of a bilayer. At the upper surface, we assume that the *A* blocks are preferred by the surface ( $F$ ) compared with the *B* blocks, i.e.,  $\gamma_{AF} < \gamma_{BF}$ . Making the above assumption implies that the *A* blocks would prefer to increase their contact area with the upper surface and, correspondingly, that the *B* blocks can decrease their contact area with the upper surface. At the bottom surface ( $S$ ), we can also have one block being preferred over the other block. We denote the interfacial tension

<sup>†</sup> Australian National University.

<sup>‡</sup> University of Sydney.

between the *A* blocks and the bottom surface by  $\gamma_{AS}$  and the *B* blocks and the bottom surface by  $\gamma_{BS}$ . Figure 1b shows a possible deformation of the lamellar interfaces, so that the contact areas of the various blocks with the upper and lower surfaces may reduce the overall free energy of the system. The *AB* interface undergoes a displacement  $u(z)$  so that the upper surface contact length of the *A* blocks is increased. In Figure 1b we assume that any two adjacent lamellar interfaces are related by  $u_{2n} = -u_{2n+1}$ , where  $n = \dots -1, 0, 1, \dots$ , and every second set of lamellar interfaces are related by  $u_n = u_{n+2}$ . This displacement is with reference to the undistorted reference state, i.e., the lamellae straight and perpendicular to the substrate. We always assume that the displacements away from the strained reference state are small, i.e.,  $u_z \ll 1$  and  $u \ll L_2/2$ . [Here  $u_z$  represents the derivative of  $u(z)$ .] As we shall see, these are very good assumptions. In this system, we assume the upper surface remains flat, which should be the case if the upper surface–diblock interfacial tensions are large compared to those of  $\gamma_{AB}$ . This is also the case if the diblock melt is confined between two hard, flat surfaces. The free energy of the lamella can be written as the sum of the chain stretching energy  $F_{stretch}$ , the *AB* interfacial energy  $F_{AB}$ , the bending energy of the lamellae  $F_{bend}$ , and the surface interfacial energy  $F_{surface}$  at the upper and lower surfaces. The term  $F_{bend}$  is caused by the distortion of the chains within the lamellae. Note that both  $F_{stretch}$  and  $F_{bend}$  arise from chain stretching entropy.  $F_{bend}$  can be calculated by slicing the lamella parallel to the *x* axis.

Consider first the stretching energy of an *AB* lamella. The stretching energy per unit length in the *y* direction is given by<sup>11</sup>

$$F_{stretch} = \frac{\pi^2 k_B T L_2}{24 N^2 a^5} \int_0^H dz (D_A^2 + D_B^2) \quad (2)$$

where  $D_A$  and  $D_B$  are the distances stretched by the *A* and *B* blocks respectively. To determine these distances, consider Figure 1b. If  $\theta$  denotes the angle between the chain, at any height  $z$ , and the horizontal, then  $D_A = [L_2/4 + u(z)]/\cos \theta$  and  $D_B = [L_2/4 - u(z)]/\cos \theta$ , where  $u(z)$  is the displacement from the unperturbed state. To obtain these expressions for  $D_A$  and  $D_B$ , we have assumed that the chain trajectories are perpendicular to the lamellar interfaces. To proceed, we assume that  $\theta$  is small and so  $\cos \theta \approx 1 - 1/2 u_z^2$ . Thus, the stretching free energy becomes, to second order in  $u$  and ignoring constant terms,

$$F_{stretch} = \frac{\pi^2 k_B T L_2^3}{24 N^2 a^5} \int_0^H dz \left[ \left( \frac{u}{L_2} \right)^2 + \frac{1}{16} u_z^2 \right] \quad (3)$$

The *AB* interfacial energy per unit length, to second order in  $u$ , is

$$F_{AB} = \gamma_{AB}/2 \int_0^H dz u_z^2 \quad (4)$$

and the energy due to bending of the lamellar interface is

$$F_{bend} = \frac{\pi^2 k_B T}{128 N^2 a^5} \left( \frac{L_2}{2} \right)^5 \int_0^H dz u_{zz}^2 \quad (5)$$

Finally the surface–diblock interfacial energy is  $F_{surface}$

$= \Delta\gamma_F u(H) + \Delta\gamma_S u(0)$ , where  $\Delta\gamma_F \equiv \gamma_{AF} - \gamma_{BF} < 0$  and  $\Delta\gamma_S \equiv \gamma_{AS} - \gamma_{BS}$ .

Putting all these terms together and using eq 1 for  $L_2$ , we obtain the total free energy per unit length in the *y* direction  $F_T$ , of one lamella as

$$F_T = \gamma_{AB} \int_0^H dz \{ 4u^2(z)/L_2^2 + 3/4 u_z^2 + 3/128 L_2^2 u_{zz}^2 \} + \Delta\gamma_F u(H) + \Delta\gamma_S u(0) \quad (6)$$

We now put this energy in dimensionless form by writing  $u(z) = L_2 f(s)$ , where  $f(s)$  is a dimensionless function of  $s = z/L_2$ . Thus, we find the dimensionless free energy  $\mathcal{F} \equiv F_T/\gamma_{AB} L_2$  is

$$\mathcal{F} = \int_0^H ds \left\{ 4f^2(s) + 3/4 \left[ \frac{df}{ds} \right]^2 + 3/128 [d^2 f/ds^2]^2 \right\} + \Delta g_F f(H) + \Delta g_S f(0) \quad (7)$$

where  $f' = df/ds$ ,  $\Delta g_F \equiv \Delta\gamma_F/\gamma_{AB}$ , and  $\Delta g_S \equiv \Delta\gamma_S/\gamma_{AB}$ .

Our main interest here is in making  $\mathcal{F}$  negative, i.e., choosing a function  $f(s)$  so that the perturbed state is lower than the unperturbed state,  $f = 0$ . To do this, we look for exact equilibrium solutions of eq 7. There is one obvious equilibrium solution,  $f(s) = 0$ , i.e., the undistorted state. The aim is to see if any other solutions exist which have a lower free energy than the undistorted state and under what conditions such solutions exist. We thus take the functional derivative of eq 7, subject to the volume constraint  $\int_0^H f(s) ds = 0$ . Thus we define the functional  $\Phi$  as

$$\Phi(f, df/ds, d^2 f/ds^2) = \mathcal{F} + \Lambda \int_0^H f(s) ds \quad (8)$$

where  $\Lambda$  is the Lagrange multiplier.<sup>12</sup> We now consider a perturbation  $\delta(s)$  to a supposed equilibrium solution,  $f_0(s)$ , i.e.,  $f(s) = f_0(s) + \delta(s)$ . Expanding  $\Phi$  to first order in  $\delta(s)$  and integrating by parts yields an expression  $\Phi = \Phi_0 + P_1 + \int_0^H ds \delta(s) \mathcal{I}[f_0(s)]$ , where  $\Phi_0$  is a constant part which we ignore,  $P_1$  arises from integrating by parts, and  $\mathcal{I}[f_0(s)]$  is a functional of  $f_0(s)$ . For  $f_0(s)$  to be an equilibrium solution, we require that terms of order  $\delta$  vanish in our expression for  $\Phi$ . This implies in particular that  $\mathcal{I}[f_0(s)] = 0$  which yields the Euler–Lagrange fourth order differential equation, from which we drop the 0 subscript:

$$\frac{3}{128} \frac{d^4 f}{ds^4} - \frac{3}{4} \frac{d^2 f}{ds^2} + 4f = -\Lambda \quad (9)$$

There are five integration constants. Thus we require five boundary conditions/constraints. Two boundary condition can be found by using the fact that we have assumed the chains are perpendicular to the *AB* interfaces. Because the upper and lower surfaces are flat, this implies that  $f_s(0) = f_s(H) = 0$ . The third and fourth boundary conditions arise from requiring that the term  $P_1$  is zero. This gives  $f_{sss}(0) = -\Delta g_S$  and  $f_{sss}(H) = \Delta g_F$ . The last constraint comes from imposing that  $\int_0^H f(s) ds = 0$  on the solution for  $f$ .

Homogeneous solutions of eq 9 are of the form  $f(s) = \exp(ms)$ . Substituting this ansatz for  $f$  into eq 9 one finds  $m^2 = 16(3 \pm \sqrt{3})/3$ . Thus, we have the general solution  $f(s) = A_1 \exp(\eta_1 s) + A_2 \exp(-\eta_1 s) + A_3 \exp(\eta_2 s) + A_4 \exp(-\eta_2 s) - \Lambda/4$ , where  $\eta_1 = 4[1 + 1/3]^{1/2} \approx 5.02$  and  $\eta_2 = 4[1 - 1/3]^{1/2} \approx 2.60$ . Here  $A_1$ ,  $A_2$ ,  $A_3$ , and  $A_4$  are constants.

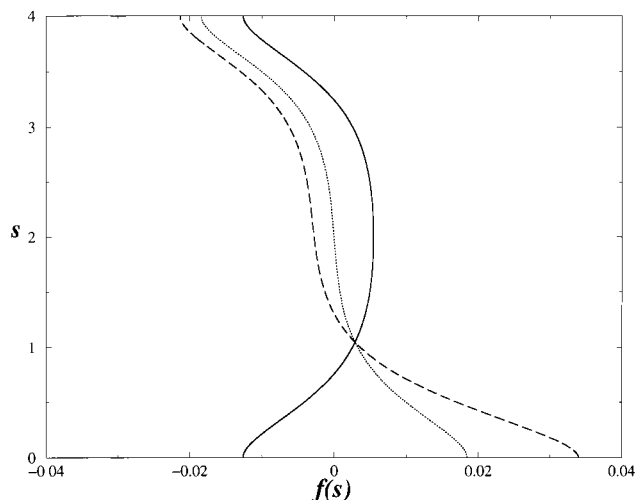


**Figure 2.** Lamellar interfaces calculated from eq 10 for a dimensionless thickness  $h = 4$  and  $\Delta g_F = \Delta g_S = 1$  (full line),  $\Delta g_F = -\Delta g_S = 1$  (dotted line), and  $\Delta g_F = 1$ ,  $\Delta g_S = -2$  (dashed line).

We first impose the volume constraint on our solutions so that the Lagrange multiplier  $\Lambda$  is determined in terms of the four other constants. We may now determine the  $A_i$ 's by applying the four boundary conditions given above. This leads to solving a matrix equation of the form  $AX = B$  where  $X$  is the vector  $(A_1, A_2, A_3, A_4)$ ,  $B$  is the vector  $(0, 0, -\Delta g_S, \Delta g_F)$ , and  $A$  is a  $4 \times 4$  square matrix. Because  $B$  is nonzero, nontrivial solutions for the  $A_i$ 's exist if  $A$  is invertible. This can be shown to occur for all thicknesses. The specific solution for any  $h$  is

$$f(s) = A_1[\exp(\eta_1 s) - 1/\eta_1 h(\exp(\eta_1 h) - 1)] + A_2[\exp(-\eta_1 s) - 1/\eta_1 h(1 - \exp(-\eta_1 h))] + A_3\left[\exp(\eta_2 s) - \frac{1}{\eta_2 h}(\exp(\eta_2 h) - 1)\right] + A_4\left[\exp(-\eta_2 s) - \frac{1}{\eta_2 h}(1 - \exp(-\eta_2 h))\right] \quad (10)$$

where  $A_1 = [\Delta g_F \exp(\eta_1 h) + \Delta g_S]/[\eta_1(\eta_1^2 - \eta_2^2)(\exp(2\eta_1 h) - 1)]$ ,  $A_2 = A_1 \exp(\eta_1 h)$ ,  $A_3 = -[\Delta g_F \exp(\eta_2 h) + \Delta g_S]/[\eta_2(\eta_1^2 - \eta_2^2)(\exp(2\eta_2 h) - 1)]$ , and  $A_4 = A_3 \exp(\eta_2 h)$ . Figure 2 shows the resulting  $AB$  lamellar interfaces for a variety of situations. Although the differences  $\Delta g_S$  and  $\Delta g_F$  are relatively large, the amplitude of the distortions are quite small, i.e., on the order of  $10^{-2}$  times the bilayer spacing. To see why this is so, we can write down explicit expressions for the distortion at the upper and lower surfaces:

$$f(h) \approx \frac{h^3}{360}(7\Delta g_S - 8\Delta g_F) \quad (11)$$

and

$$f(0) \approx \frac{h^3}{360}(7\Delta g_F - 8\Delta g_S) \quad (12)$$

These expressions are found by taking the first term in a Taylor series about  $h = 0$ . In each case, the effect is drastically reduced by a very small numerical prefactor  $1/360$ . In the opposite limit of very thick films, the expressions are

$$f(h) \approx -\Delta g_F/[\eta_1 \eta_2 (\eta_1 + \eta_2)] \approx -0.01 \Delta g_F \quad (13)$$

$$f(0) \approx -\Delta g_S/[\eta_1 \eta_2 (\eta_1 + \eta_2)] \approx -0.01 \Delta g_S \quad (14)$$

Thus, although there are very good physical reasons for the distortion shown in Figure 1b to occur, the amplitude is always very small. Note that this instability will occur for all systems provided either  $\Delta g_S$  or  $\Delta g_F$  is nonzero and the amplitude of the instability is linearly related to the differences in surface tensions.

### 3 Distorted Perpendicular versus Parallel Morphology

When a diblock copolymer melt thin film forms on a flat surface, or between two flat surfaces, the lamellae may orientate themselves either parallel or perpendicularly to the surface.<sup>1,2</sup> For perpendicular orientation, we have just seen that distortions of the lamellar interfaces will lower the free energy of the system. We now want to know how the free energy of this configuration compares with the free energy of a parallel morphology. To make this comparison, we need to calculate the free energy of the perpendicular morphology and the parallel morphology and then compare them. The difference in free energy per unit length in the  $y$  direction between the undistorted perpendicular and parallel morphologies, of length  $L_2/2$  in the  $x$  direction,  $\mathcal{F}_1 = F_{10} - F_{10}$  is given by<sup>2</sup>

$$\mathcal{F}_1 = 1/2[(h^3/n_l^2) + 2n_l - 3h + 1/2(\pm\Delta g_S \pm \Delta g_F)] \quad (15)$$

where  $n_l = n$  for a parallel symmetric morphology (i.e.,  $AB...BA$  or  $BA...AB$ ) and  $n_l = n + 1/2$  for a parallel antisymmetric morphology (i.e.,  $AB...AB$  or  $BA...BA$ ), and  $n \in I$ . The reason we have the  $\pm$  symbol in the above equation is that the free energy of the parallel state must be minimized between symmetric and antisymmetric states. Because we know that our distorted perpendicular state always has lower free energy than the undistorted perpendicular state, we only need to compare our state with the parallel orientation. This is done by calculating the free energy difference  $\Delta G \equiv \mathcal{F} - \mathcal{F}_1$ , and when  $\Delta G < 0$ , our distorted perpendicular state is observed. Figure 3, which is calculated for  $\Delta g_F = \Delta g_S = -0.15$ , shows that the distorted perpendicular orientation occurs for relatively thin films. In fact, the absolute value of  $\mathcal{F}$ , given by eq 7, is much smaller than the energy of the undistorted perpendicular morphology. Thus, the effect of the distortions on the phase diagram is relatively small; i.e., the region of parallel alignment of the lamellae is not too different from that calculated by Walton *et al.*<sup>2</sup> It might be thought that we could increase the amplitude of our instability by increasing the values of the interfacial tension differences  $\Delta g_F$  and  $\Delta g_S$ . However, when these become large, the system reverts to the parallel orientation.

Before concluding, we will comment on a few other studies of thin film diblock melts. Recently, Matsen<sup>13</sup> has used a numerical self-consistent mean-field theory to determine the equilibrium morphology of confined films. In that study, he found evidence for parallel, perpendicular, and mixed lamellar morphologies. A mixed morphology has parallel lamellae at one surface and perpendicular lamellae near the other surface. Therefore, a junction exists between the two morphologies, which costs extra interfacial energy. Matsen<sup>13</sup> concluded that for symmetrical diblocks the mixed state

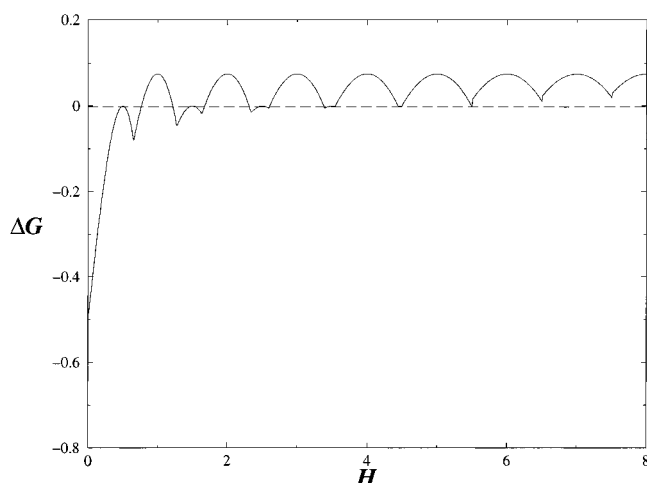


**Figure 3.** Plot of  $\Delta G$  versus  $H/L_2$  for  $\Delta g_S = \Delta g_F = -0.15$ .  $\Delta G < 0$  is where undulations occur.

was unstable compared to the parallel and perpendicular state and that these mixed lamellae may be observed because they are kinetically favored, rather than the equilibrium structure. This observation is supported by recent experimental studies of Mansky *et al.*,<sup>14</sup> who found evidence for mixed lamellar morphologies but also found that over time they decayed away. In fact, we may carry out a simple free energy analysis to show in the case of symmetrical plates, i.e. the case in Figure 3, that the mixed lamellar morphology is never favored compared to the perpendicular and parallel morphologies. Other recent studies by Morkved and Jaeger<sup>15</sup>, Fasolka *et al.*,<sup>16</sup> and Tang and Witten,<sup>17</sup> although carried out for thin films, are not precisely for the same conditions that we assume. For example, all of these studies allow the thickness of the film to vary. In this case, the strain in the system may be relieved by the formation of other types of morphologies, i.e., teardrop type structures or cylinders perforating the lamellae. The main point to be made about these studies is that the morphologies determined are not necessarily the true equilibrium

morphologies but rather metastable ones, albeit with very slow kinetics.

In summary, we have shown that thin films of symmetric diblocks aligned perpendicular to the substrate will always show a periodic distortion like that shown in Figure 1b. However, this distortion will always be of very small amplitude on the order of a few percent of the bilayer spacing. Such distortions have been observed in recent numerical simulations<sup>5,8,13</sup> and may be observable in careful experiments.

**Acknowledgment.** G.G.P. and D.R.M.W. acknowledge support from an ARC Large Grant and D.R.M.W. is supported by an ARC QEII.

## References and Notes

- (1) Turner, M. S. *Phys. Rev. Lett.* **1992**, *69*, 1788.
- (2) Walton, D. G.; Kellog, G. J.; Mayes, A. M.; Lambooy, P.; Russell, T. P. *Macromolecules* **1994**, *27*, 6225.
- (3) Coulon, G.; Collin, B.; Ausserre, D.; Chatenay, D.; Russell, T. P. *J. Phys. (Paris)* **1990**, *51*, 2801. Mansky, P.; Liu, Y.; Huang, E.; Russell, T. P.; Hawker, C. *Science* **1997**, *275*, 1458.
- (4) Coulon, G.; Collin, B.; Chatenay, D.; Gallot, Y. *J. Phys. II* **1993**, *3*, 697.
- (5) Pickett, G. T.; Balazs, A. C. *Macromolecules* **1997**, *30*, 3097. Pickett, G. T.; Balazs, A. C. *Macromol. Theory Sim.* **1998**, *7*, 249.
- (6) Williams, D. R. M. *Phys. Rev. Lett.* **1995**, *75*, 7677.
- (7) Heier, J.; Kramer, E. J.; Walheim, S.; Krausch, G. *Macromolecules* **1997**, *30*, 6610.
- (8) Matsen, M. W. *Curr. Opin. Colloid Interface Sci.* **1998**, *3*, 40.
- (9) Petera, D.; Muthukumar, M. *J. Chem. Phys.* **1997**, *107*, 9640.
- (10) Bates, F. S.; Fredrickson, G. H. *Annu. Rev. Phys. Chem.* **1990**, *41*, 525.
- (11) Wang, Z.-G. *J. Chem. Phys.* **1994**, *100*, 229. Milner, S. T.; Witten, T. A. *J. Phys. (Paris)* **1988**, *49*, 1951.
- (12) Forray, M. J. *Variational Calculus in Science and Engineering*; McGraw-Hill Book Company: New York, 1968; p 65.
- (13) Matsen, M. W. *J. Chem. Phys.* **1997**, *106*, 7781.
- (14) Mansky, P.; Russell, T. P.; Hawker, C. J.; Pitsakalis, M.; Mays, J. *Macromolecules* **1997**, *30*, 6810.
- (15) Morkved, T. L.; Jaeger, H. M. *Europhys. Lett.* **1997**, *40*, 643.
- (16) Fasolka, M. J.; Harris, D. J.; Mayes, A. M.; Yoon, M.; Mochrie, S. G. *J. Phys. Rev. Lett.* **1997**, *79*, 3018.
- (17) Tang, W. H.; Witten, T. A. *Macromolecules* **1998**, *31*, 3135.

MA981120I